Journal of Power Sources 202 (2012) 352–356

Contents lists available at SciVerse ScienceDirect

Journal of Power Sources

journal homepage: www.elsevier.com/locate/jpowsour

Short communication

Synthesis of $LiCoMnO_4$ via a sol–gel method and its application in high power $LiCoMnO_4/Li_4Ti_5O_{12}$ lithium-ion batteries

Xingkang Huang[a,*], Min Lin[a], Qingsong Tong[a], Xiuhua Li[a], Ying Ruan[a], Yong Yang[b,**]

[a] Department of Chemistry, Fujian Normal University, Fuzhou 35007, PR China
[b] State Key Lab for Physical Chemistry of Solid Surfaces, Department of Chemistry, Xiamen University, Xiamen 361005, PR China

ARTICLE INFO

Article history:
Received 10 August 2011
Received in revised form 12 October 2011
Accepted 10 November 2011
Available online 20 November 2011

Keywords:
Lithium manganese oxide
5 V spinel
Lithium titanium oxide
Lithium-ion battery

ABSTRACT

A $LiCoMnO_4$ (5 V spinel) material has been synthesized by annealing a sol–gel precursor utilizing lithium acetate, cobalt acetate, manganese acetate, and citric acid. The as-prepared sample has been determined to be $LiCo_{1.09}Mn_{0.91}O_4$ via inductive coupled plasma-atomic emission spectroscopy. The deviation of the molar ratio of Co/Mn from 1:1 is designed to minimize the amount of $LiMn_2O_4$ impurity in our sample. The produced spinel material possesses an initial discharge capacity of 87.1 mAh g^{-1} with two voltage plateaus at 5.1 and 4.9 V. The $LiCo_{1.09}Mn_{0.91}O_4$ cathode has been assembled with a $Li_4Ti_5O_{12}$ anode to form a full-cell which delivered a discharge capacity of 131.2 mAh g^{-1}, centered at 3.2 V. It is of great interest that despite the low coulombic efficiency of the full-cell, it shows good cyclic performance. In addition, The $LiCo_{1.09}Mn_{0.91}O_4/Li_4Ti_5O_{12}$ cell shows an excellent rate capability, delivering a capacity of 84.2 mAh g^{-1}, corresponding to a high power density of 4.70 kW kg^{-1} at the current density of 1700 mA g^{-1}.

1. Introduction

High power lithium-ion batteries have attracted a lot of interest in recent years, especially as devices for electrical vehicles (EVs) and hybrid electrical vehicles (HEVs). Because of safety issues, $LiFePO_4$ has been regarded as one of the most promising cathodes for lithium-ion batteries in the practical application for EVs and HEVs, where, however, the commonly used anode material, graphite, remains a latent danger due to its flammability. Therefore, $Li_4Ti_5O_{12}$ anodes were employed to develop non-flammable $LiFePO_4/Li_4Ti_5O_{12}$ Li-ion batteries [1,2]. The $LiFePO_4/Li_4Ti_5O_{12}$ batteries exhibit voltage plateau of ca. 1.85 V only, which is much lower than general lithium-ion batteries (ca. 3.7 V). To utilize the non-flammability of $Li_4Ti_5O_{12}$ without losing the advantages associated with the high voltage of lithium-ion batteries, high voltage cathode materials such as $LiNi_{0.5}Mn_{1.5}O_4$ were employed to substitute for $LiFePO_4$ cathodes [3–5]. $LiNi_{0.5}Mn_{1.5}O_4$ is a 5 V spinel, possessing a potential plateau of ca. 4.7 V versus Li^+/Li, and showing ca. 3.1 V voltage plateau when using $Li_4Ti_5O_{12}$ as an anode. Considering that $LiCoMnO_4$ has an even higher potential than $LiNi_{0.5}Mn_{1.5}O_4$ (ca. 5.0 V versus Li^+/Li), we fabricated a $LiCoMnO_4/Li_4Ti_5O_{12}$ battery and investigated its electrochemical performance.

$LiCoMnO_4$ possesses a spinel structure similar to that of $LiMn_2O_4$ with a space group of $Fd\bar{3}m$, where the Co^{3+} and Mn^{4+} are distributed in 16d sites randomly or in a short ordering which is dependent on the temperature and cooling rate used during this synthesis [6]. Compared to half of Mn atoms in $LiMn_2O_4$ being an active couple, all Mn elements in $LiCoMnO_4$ are fixed as +4 while cobalt atoms vary between Co^{3+} and Co^{4+} during charging/discharging. Unlike the extensive investigation that already exists on $LiNi_{0.5}Mn_{1.5}O_4$ [7–11], currently, there are much less reports in the literature concerned with $LiCoMnO_4$ [6,12–15]. In 1998, Kawai et al. synthesized a $LiCoMnO_4$ by a solid-state reaction, showing a discharge capacity of ca. 102 mAh g^{-1}. From then on, few investigations could be found on the electrochemical performance of $LiCoMnO_4$ materials. This lack of investigation into $LiCoMnO_4$ may be due to electrolyte decomposition caused by the potential being too high for electrolytes used at that time. Considering the recent developments in the non-aqueous electrolytes, which provide improved tolerance of high potentials, the electrochemical performance of $LiCoMnO_4$ is worthy of being re-examined. Therefore, in order to develop a non-flammable, high power lithium-ion battery, we synthesized $LiCoMnO_4$ via a sol–gel method and investigated its electrochemical performance in lithium-ion batteries using $Li_4Ti_5O_{12}$ as an anode material.

2. Experimental

The $LiCoMnO_4$ material was synthesized by a sol–gel method. A 150 mL solution containing 2.754 g $Co(CH_3COO)_2{\cdot}4H_2O$, 2.256 g

* Corresponding author. Tel.: +86 591 83439030.
** Corresponding author. Tel.: +86 592 2185753; fax: +86 592 2185753.
E-mail addresses: xkhuang@126.com (X. Huang), yyang@xmu.edu.cn (Y. Yang).

0378-7753/$ – see front matter © 2011 Elsevier B.V. All rights reserved.
doi:10.1016/j.jpowsour.2011.11.028

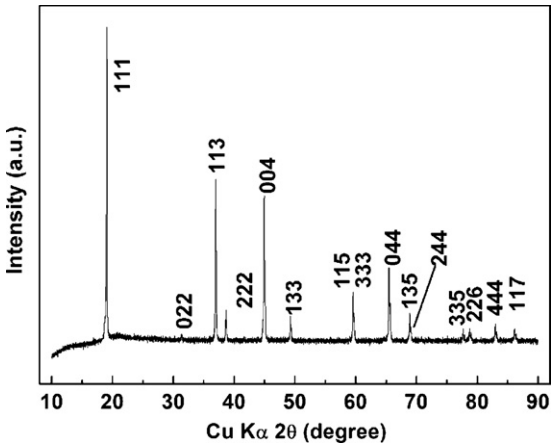

Fig. 1. XRD pattern of the as-prepared sample.

$Mn(CH_3COO)_2{\cdot}4H_2O$, 1.061 g $LiCH_3COO{\cdot}2H_2O$, and 8.448 g citric acid ($C_6H_8O_7{\cdot}H_2O$), was stirred and heated at 90 °C until forming a xerogel. The xerogel was heated in a muffle furnace at 380 °C for 10 h, and then annealed under O_2 atmosphere at 800 °C for 24 h, where the heating and cooling rates above 400 °C were set to be 1 °C min^{-1}.

The as-prepared sample was examined by powder X-ray diffraction (XRD) analysis, performed using a PANalytical X'Pert diffractometer with Cu Kα radiation (Philips). Morphology observation was studied by scanning electron microscopy (SEM) performed on a Hitachi S-4800. The Co, Mn, and Li contents were determined by inductive coupled plasma-atomic emission spectroscopy (ICP-AES), carried out on IRIS Intrepid II XSP (Thermo Electron).

Electrode fabrication and coin cell assembly were carried out as described in our previous report [16]. In brief, the active material was mixed with 10 wt% acetylene black and 10 wt% binder (PVDF), and then ground by ball milling. The cathode was obtained by pressing the mixture onto a piece of aluminum foil followed by drying in a vacuum oven at 120 °C for 2 h. The coin cells were fabricated with the prepared cathode, lithium anode, Celgard 2400 polypropylene separator, and 1 M LPF_6 in EC/DMC (1:1, v/v) electrolyte. The $Li_4Ti_5O_{12}$ anode was employed to replace the lithium anode when assembling a $LiCoMnO_4/Li_4Ti_5O_{12}$ cell, where some stainless components were often introduced in order to remove the trouble of loose touch between the cathode, separator, and anode. The fabrication procedures of a $Li_4Ti_5O_{12}$ anode were exactly the same as those used for the $LiCoMnO_4$ cathode. The $Li_4Ti_5O_{12}$ used was kindly provided by the BTR New Energy Material Co., Ltd. Cell testing was carried out at constant current densities at 27 °C using a Land battery test system (Wuhan, China).

3. Results and discussion

The XRD pattern of the as-prepared sample is shown in Fig. 1, where all the peaks were indexed to the spinel structure with a space group of $Fd\bar{3}m$. The lattice parameter a of the sample was calculated to be 0.80556 nm, smaller than those of $LiMn_2O_4$ (0.82438 nm) [17] and $Li_2CoMn_3O_8$ (0.81379 nm) [18]. This result is in good agreement with the fact that the cobalt ion (III) possesses a smaller radius than the manganese ion (III). The contents of Li, Co, and Mn in the sample were determined by ICP-AES and the formula of such a sample was calculated to be $LiCo_{1.09}Mn_{0.91}O_4$. The molar ratio of Co/Mn as 109:91 is designed to reduce the discharge capacity at ca. 4 V as detailed in the electrochemical discussion (below). Well-defined particles were observed for this sample synthesized at 800 °C (Fig. 2). The average particle size produced is ca. 200 nm,

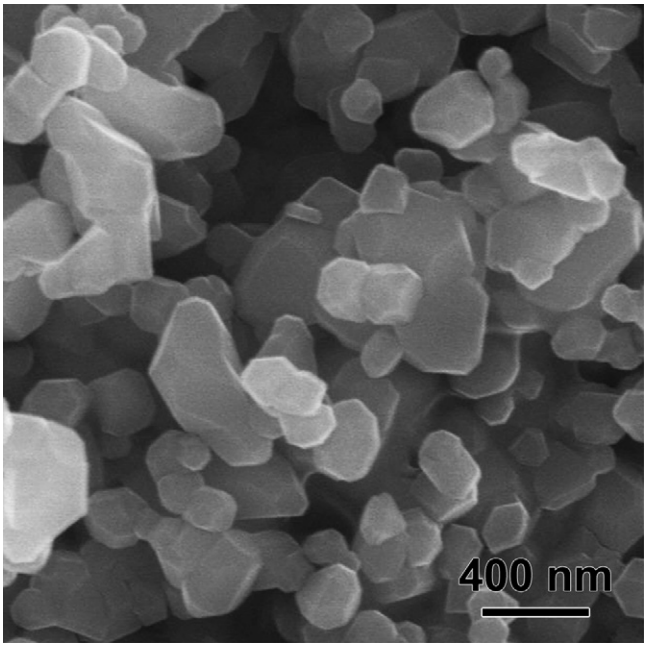

Fig. 2. SEM image of the as-prepared sample.

similar to those of $LiNi_{0.5}Mn_{1.5}O_4$ materials synthesized via the sol–gel method [10,11,19].

The charge/discharge curves of the $LiCo_{1.09}Mn_{0.91}O_4$ during the initial five cycles are presented in Fig. 3. The $LiCo_{1.09}Mn_{0.91}O_4$ exhibits two plateaus at 4.9 and 5.1 V with a discharge capacity of ca. 87.1 mAh g^{-1}. The coulombic efficiency of the $LiCo_{1.09}Mn_{0.91}O_4$ is low, especially for the initial cycle, which mainly resulted from decomposition of the electrolyte at high potentials upon charging to 5.3 V.

Kawai et al. [13] synthesized a $LiCoMnO_4$ material by a solid state reaction at 800 °C which yielded a discharge capacity of ca. 95 mAh g^{-1}, centered at 5.0 V, and showed ca. 10 mAh g^{-1} at the plateau of 4 V. Mandal et al. [20] prepared a $LiCoMnO_4$ material delivering a capacity of ca. 90 mAh g^{-1} (ca. 20 mAh g^{-1} below 4.3 V). By contrast, our sample delivered a discharge capacity of 87.1 mAh g^{-1}, and the 4 V discharge plateau was negligible (Fig. 3). Note here that the molar ratio of Co/Mn in our material was set to be 109:91, due to a ratio of 1:1 resulting in a capacity of ca. 10 mAh g^{-1} at 4 V plateau. The 4 V plateau is associated with the

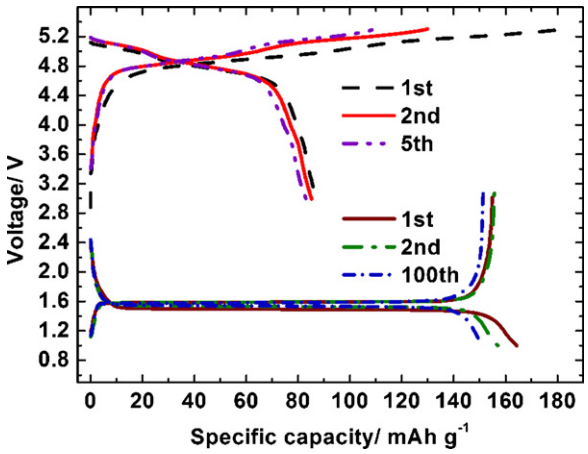

Fig. 3. Charge–discharge curves of $LiCo_{1.09}Mn_{0.91}O_4$ (above) and $Li_4Ti_5O_{12}$ (below) at current densities of 140 and 170 mA g^{-1}, respectively; lithium anodes were employed for both cathodes.

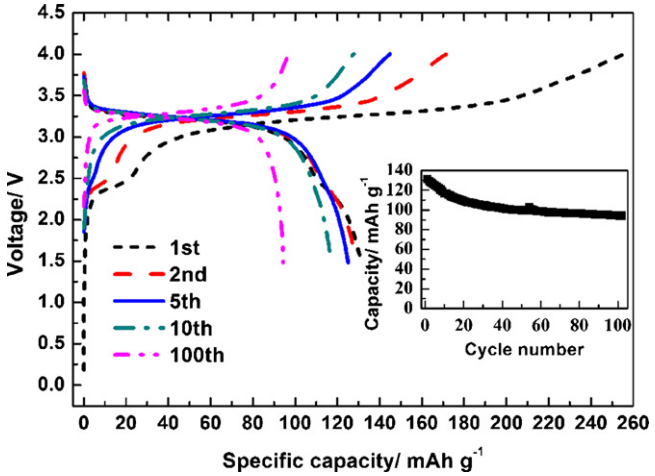

Fig. 4. Charge/discharge curves of $LiCo_{1.09}Mn_{0.91}O_4/Li_4Ti_5O_{12}$ cell at a current density of 170 mA g^{-1} (calculated based on the mass of $Li_4Ti_5O_{12}$); the inset shows its cyclic performance.

Mn^{3+} that is present in the impurity phase of $LiMn_2O_4$, which is commonly suffered from Jahn–Teller disorder of MnO_6 octahedron upon electrochemically cycling. Such a disorder could be suppressed by partly substituting Mn using divalent or trivalent metal ions (such as Mg, Cu, Ni, Cr, Al, Co, Ga) [21–25]. Considering cobalt possesses a valence state of +3 in the $LiCoMnO_4$, we therefore employ cobalt to partly replace manganese in order to suppress the formation of Mn^{3+} during synthesis of $LiCoMnO_4$ materials. The ratio of 109:91 for Co/Mn is an optimized value; over-substituting of Mn would result in formation of impurities of cobalt oxides and reduce the discharge capacity.

Before assembling a full-cell of $LiCo_{1.09}Mn_{0.91}O_4/Li_4Ti_5O_{12}$, the $Li_4Ti_5O_{12}$ anode was examined. As shown in Fig. 3, the $Li_4Ti_5O_{12}$ delivered a capacity of ca. 160 mAh g^{-1} and presented an excellent cyclic stability. Therefore, $LiCo_{1.09}Mn_{0.91}O_4/Li_4Ti_5O_{12}$ should be designed on the basis of the capacity limited by $Li_4Ti_5O_{12}$, which is consistent with the result of Xiang et al. [4]; their results show that cells with their capacity limited by $Li_4Ti_5O_{12}$ exhibited better cyclic performance than those limited by $LiNi_{0.5}Mn_{1.5}O_4$. Consequently, the capacities of $LiCo_{1.09}Mn_{0.91}O_4$ electrodes were then selected to be roughly double those of the $Li_4Ti_5O_{12}$ electrodes. The $LiCo_{1.09}Mn_{0.91}O_4/Li_4Ti_5O_{12}$ cell possessed a voltage plateau of ca. 3.2 V and delivered an initial discharge capacity of 131.2 mAh g^{-1} at 170 mA g^{-1} (Fig. 4). After 20 cycles, its capacity decayed to 109.1 mAh g^{-1}, and then stabilized at ca. 100 mAh g^{-1}; after additional 80 cycles, its capacity remained at 94.4 mAh g^{-1}. The capacity decay of the full-cell at the early stage is associated with both cathode and anode, where the anode fading should not result from the degeneration of the $Li_4Ti_5O_{12}$ material itself, but possibly from side reactions at the anode upon charging, which is still under investigation.

When charged, $LiCo_{1.09}Mn_{0.91}O_4$ turned to $Li_{1-x}CoMnO_4$, accompanied with transformation of $Li_{4/3}Ti_{5/3}O_4$ (another form of $Li_4Ti_5O_{12}$) into $Li_{4/3+y}Ti_{5/3}O_4$. Interestingly the initial charging capacity of $LiCo_{1.09}Mn_{0.91}O_4/Li_4Ti_5O_{12}$ is as high as 255.6 mAh g^{-1} (Fig. 4), well beyond the theoretical capacity of $Li_4Ti_5O_{12}$ (175 mAh g^{-1}). This means that there is at least one additional reaction which occurs on the anode upon charging. The additional side reaction is uncertain at the present stage; however, it is believed that some species, formed at the cathode (e.g., decomposition of the electrolyte), were then reduced at the anode while charging. Considering the existence of side reactions at both electrodes, x in $Li_{1-x}CoMnO_4$ is not equal to y in $Li_{4/3+y}Ti_{5/3}O_4$. In the initial discharge processes, the presence of the plateau at 2.6 V

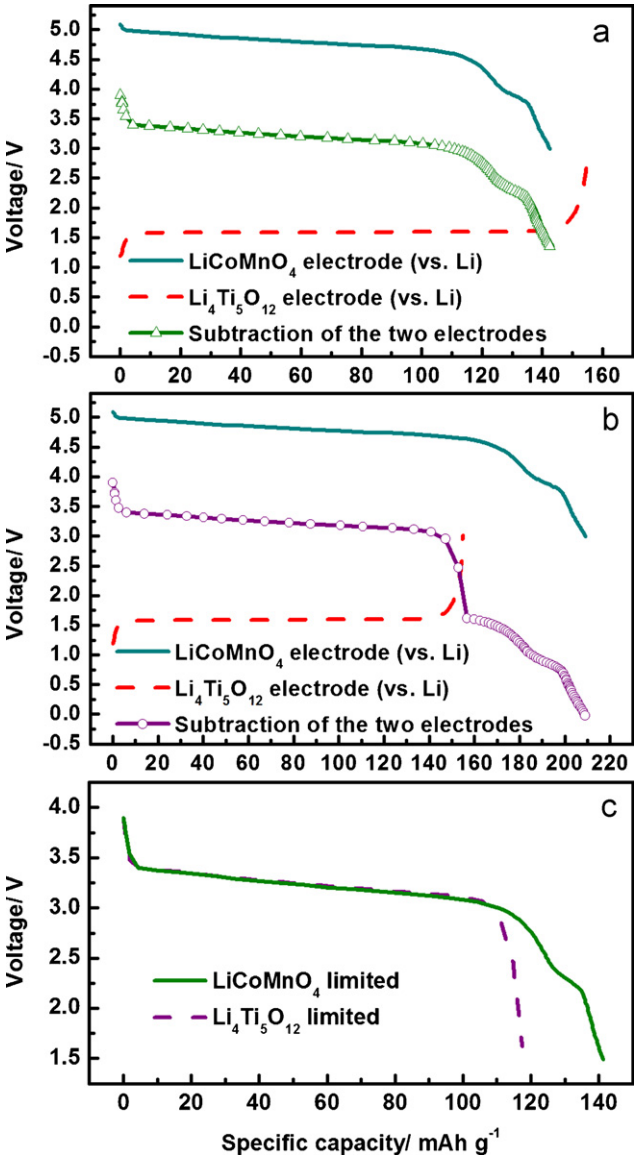

Fig. 5. Simulation of discharging processes of $LiCoMnO_4/Li_4Ti_5O_{12}$ full cells with capacity limited by (a) $LiCoMnO_4$ and (b) $Li_4Ti_5O_{12}$; (c) discharge curves of the batteries with capacity limited by the $LiCoMnO_4$ and $Li_4Ti_5O_{12}$ electrode. Note that the capacities of the $LiCoMnO_4$ electrodes shown in (a) and (b) are results from a measured value multiplied by some coefficients, in order to obtain suitable cathode curves to be subtracted by the anode curve for simulation.

(corresponding to the 4 V plateau of the cathode) indicates that x is smaller than y (Fig. 4), consequently presenting discharge curves similar to those of the $LiCo_{1.09}Mn_{0.91}O_4$/Li cell with poor cycleability. Due to the low coulombic efficiency of the $LiCo_{1.09}Mn_{0.91}O_4$ electrode the x gradually became greater than y with repeated charge/discharge. As a result, the full-cell behaved like $Li_4Ti_5O_{12}$/Li, showing no plateau at 4 V and presenting good cyclic performance.

In order to describe the difference in the cyclic performances of the two batteries with discharging capacity limited by $LiCoMnO_4$ and $Li_4Ti_5O_{12}$, a discharge curve of a $LiCoMnO_4$ (versus Li) was subtracted by that of the $Li_4Ti_5O_{12}$ to simulate discharge behaviors of the $LiCoMnO_4/Li_4Ti_5O_{12}$ full cell. The original discharge curve of the $LiCoMnO_4$ employed here is attributed to the material synthesized in the presence of Co/Mn molar ratio of 1:1, where a remarkable 4 V plateau was observed. As shown in Fig. 5a, the full cell with its capacity limited by $LiCoMnO_4$, has an additional plateau appearing at 4 V associated with the impurity phase of $LiMn_2O_4$. By contrast,

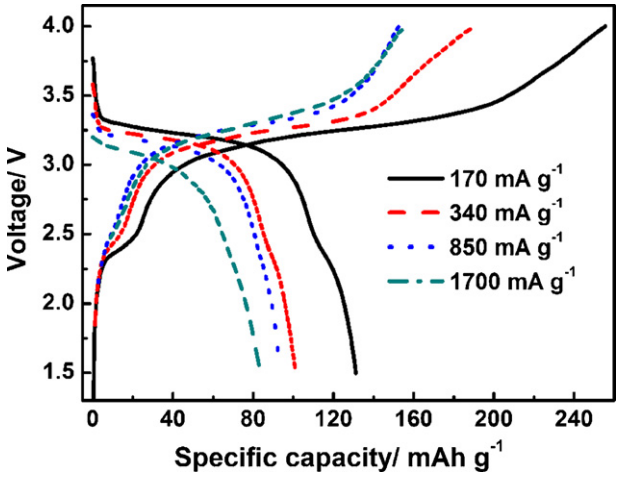

Fig. 6. Charge/discharge curves of $LiCo_{1.09}Mn_{0.91}O_4/Li_4Ti_5O_{12}$ cells at various currents.

when the full cell is limited in capacity by $Li_4Ti_5O_{12}$, the 4 V plateau of the cathode could not be obtained because it requires a cutoff below 1.5 V as depicted in Fig. 5b.

A comparison of discharge processes for full cells with their capacity limited by $LiCoMnO_4$ and by $Li_4Ti_5O_{12}$ is shown in Fig. 5c. The capacity limited by $Li_4Ti_5O_{12}$ was multiplied by 0.75 to simulate the switching process limited by from $LiCoMnO_4$ to $Li_4Ti_5O_{12}$. This simulation is very close to the cyclic process of the $LiCo_{1.09}Mn_{0.91}O_4/Li_4Ti_5O_{12}$ cell shown in Fig. 4, where the cell was limited by $LiCo_{1.09}Mn_{0.91}O_4$ and $Li_4Ti_5O_{12}$ at the early and late stages, respectively. Such a transformation process of capacity limited by from a cathode into an anode was also observed in a $LiNi_{0.5}Mn_{1.5}O_4/Li_4Ti_5O_{12}$ battery recently, where the initial capacity of ca. 30 mAh g^{-1} at ca. 2.6 V plateau disappeared progressively upon 40 cycles while its capacity located at ca. 3 V developed gradually from ca. 90 into 120 mAh g^{-1} (not shown here).

A $LiCo_{1.09}Mn_{0.91}O_4/Li_4Ti_5O_{12}$ full cell cycled with capacity limited by $Li_4Ti_5O_{12}$, would result in a shallow depth of discharge for the $LiCo_{1.09}Mn_{0.91}O_4$. It is well known that an electrode material possesses better cyclic performance if it is charged and discharged in a shallow depth. Meanwhile, considering the $Li_4Ti_5O_{12}$ has very good capacity retention (Fig. 3), it is not surprising that the full cell shows very good cyclic performance when its capacity was limited by $Li_4Ti_5O_{12}$. Unlike lithium-ion batteries with carbon anodes which require the anode capacity in excess in order to operate safely without malfunction, it is of safe that a $LiCoMnO_4/Li_4Ti_5O_{12}$ cell with the cathode capacity in excess does not result in deposition of Li on the surface of the anode and hence does not lead to the same safety hazard.

The $LiCo_{1.09}Mn_{0.91}O_4/Li_4Ti_5O_{12}$ cell presents a very good rate capability as shown in Fig. 6. At current densities of 170, 340, 850, and 1700 mA g^{-1}, the discharge capacities of the $LiCo_{1.09}Mn_{0.91}O_4/Li_4Ti_5O_{12}$ cells are 131.2, 101.0, 93.4, and 84.2 mAh g^{-1}, corresponding to the power densities of 0.51, 1.01, 2.50, 4.70 kW kg^{-1}, respectively. Consequently, the $LiCo_{1.09}Mn_{0.91}O_4/Li_4Ti_5O_{12}$ cell is of great potential in the application of high power lithium-ion batteries.

4. Conclusion

$LiCo_{1.09}Mn_{0.91}O_4$ was synthesized via a sol–gel method, followed by annealing at 800 °C. The as-prepared sample possesses a spinel structure with a mean particle size of ca. 200 nm. Such a spinel showed an initial discharge capacity of 87.1 mAh g^{-1} with two voltage plateaus at 5.1 and 4.9 V. The plateau at ca. 4.0 V is negligible, which indicates that the impurity phase of $LiMn_2O_4$, normally observed in previously reported samples, is also negligible in our sample. This optimized result was achieved by partly substituting manganese with cobalt to suppress the formation of Mn^{3+} in the form of $LiMn_2O_4$.

The $LiCo_{1.09}Mn_{0.91}O_4$ was assembled with a $Li_4Ti_5O_{12}$ anode to be a full-cell. The full-cell delivered a discharge of 131.2 mAh g^{-1}, centered at 3.2 V. It is of great interest that despite the low coulombic efficiency of the full-cell, it still shows a good cyclic performance. At the initial cycling stages the full-cell presented a discharge curve with a capacity limited by $LiCo_{1.09}Mn_{0.91}O_4$ electrode, while at subsequent stages (after about 20 cycles) the cell acted as $Li_4Ti_5O_{12}$ limited upon discharging to 1.5 V. The $LiCo_{1.09}Mn_{0.91}O_4/Li_4Ti_5O_{12}$ cell shows a very good rate capability, delivering a capacity of 84.2 mAh g^{-1}, corresponding to a high power density of 4.70 kW kg^{-1} at the current density of 1700 mA g^{-1}.

Acknowledgements

This work is supported by Science and Technology Project from the Educational Commission of Fujian Province, China (grant no. JA10072), Grant for Distinguish Young Scholar in Universities of Fujian Province, China (no. JA11040), and Science Foundation of Fujian Province, China (grant no. 2011J05021). Y.Y. gratefully acknowledges the financial support from the National Basic Research Program of China (973 Program) (grant no. 2007CB209702), and the National Natural Science Foundation of China Grants (nos. 20473060, 29925310, and 20021002). Y.R. thanks Creative Experiments Project for Undergraduate Students of Fujian Province, China (no. Fjnu2011-022). The authors also thank the BTR New Energy Material Co., Ltd. for kindly providing the $Li_4Ti_5O_{12}$ sample.

References

[1] A. Jaiswal, C.R. Horne, O. Chang, W. Zhang, W. Kong, E. Wang, T. Chern, M.M. Doeff, J. Electrochem. Soc. 156 (2009) A1041–A1046.
[2] J. Morales, R. Trocoli, S. Franger, J. Santos-Pena, Electrochim. Acta 55 (2010) 3075–3082.
[3] H.M. Wu, I. Belharouak, H. Deng, A. Abouimrane, Y.K. Sun, K. Amine, J. Electrochem. Soc. 156 (2009) A1047–A1050.
[4] H.F. Xiang, X. Zhang, Q.Y. Jin, C.P. Zhang, C.H. Chen, X.W. Ge, J. Power Sources 183 (2008) 355–360.
[5] H.F. Xiang, Q.Y. Jin, R. Wang, C.H. Chen, X.W. Ge, J. Power Sources 179 (2008) 351–356.
[6] R.K. Stoyanova, E.N. Zhecheva, M.Y. Gorova, J. Mater. Chem. 10 (2000) 1377–1381.
[7] R. Santhanam, B. Rambabu, J. Power Sources 195 (2010) 5442–5451.
[8] X.K. Huang, Q.S. Zhang, J.L. Gan, H.T. Chang, Y. Yang, J. Electrochem. Soc. 158 (2011) A139–A145.
[9] D.C. Li, A. Ito, K. Kobayakawa, H. Noguchi, Y. Sato, Electrochim. Acta 52 (2007) 1919–1924.
[10] J.Y. Shi, C.W. Yi, K. Kim, J. Power Sources 195 (2010) 6860–6866.
[11] T.F. Yi, C.Y. Li, Y.R. Zhu, J. Shu, R.S. Zhu, J. Solid State Electrochem. 13 (2009) 913–919.
[12] H. Kawai, M. Nagata, H. Kageyama, H. Tukamoto, A.R. West, Electrochim. Acta 45 (1999) 315–327.
[13] H. Kawai, M. Nagata, H. Tukamoto, A.R. West, Electrochem, Solid State Lett. 1 (1998) 212–214.
[14] D. Pasero, S. de Souza, N. Reeves, A.R. West, J. Mater. Chem. 15 (2005) 4435–4440.
[15] E. Zhecheva, R. Stoyanova, R. Alcantara, P. Lavela, J.L. Tirado, J. Power Sources 159 (2006) 1389–1394.
[16] X.K. Huang, Q.S. Zhang, H.T. Chang, J.L. Gan, H.J. Yue, Y. Yang, J. Electrochem. Soc. 156 (2009) A162–A168.
[17] K. Oikawa, T. Kamiyama, F. Izumi, D. Nakazato, H. Ikuta, M. Wakihara, J. Solid State Chem. 146 (1999) 322–328.
[18] P. Strobel, A. Ibarra Palos, M. Anne, F. Le Cras, J. Mater. Chem. 10 (2000) 429–436.
[19] H.Y. Xu, S. Xie, N. Ding, B.L. Liu, Y. Shang, C.H. Chen, Electrochim. Acta 51 (2006) 4352–4357.
[20] S. Mandal, R.M. Rojas, J.M. Amarilla, P. Calle, N.V. Kosova, V.F. Anufrienko, J.M. Rojo, Chem. Mater. 14 (2002) 1598–1605.

[21] D. Capsoni, M. Bini, G. Chiodelli, V. Massarotti, P. Mustarelli, L. Linati, M.C. Mozzati, C.B. Azzoni, Solid State Commun. 126 (2003) 169–174.
[22] D. Capsoni, M. Bini, G. Chiodelli, P. Mustarelli, V. Massarotti, C.B. Azzoni, M.C. Mozzati, L. Linati, J. Phys. Chem. B 106 (2002) 7432–7438.
[23] R. Thirunakaran, B.R. Babu, N. Kalaiselvi, P. Periasamy, T.P. Kumar, N.G. Renganathan, M. Raghavan, N. Muniyandi, Bull. Mater. Sci. 24 (2001) 51–55.
[24] M. Okada, Y.S. Lee, M. Yoshio, J. Power Sources 90 (2000) 196–200.
[25] R. Basu, R. Seshadri, J. Mater. Chem. 10 (2000) 507–510.